

MINI-RF BISTATIC OBSERVATIONS OF COPERNICAN CRATER EJECTA. A. M. Stickle¹, G. W. Patterson¹, J. T. S. Cahill¹, P. Prem¹, and the Mini-RF team¹ Johns Hopkins Applied Physics Laboratory, 11100 Johns Hopkins Rd., Laurel, MD, USA 20723, angela.stickle@jhuapl.edu.

Introduction: The Mini-RF instrument onboard NASA's Lunar Reconnaissance Orbiter (LRO) is currently acquiring bistatic radar data of the lunar surface at both S-band (12.6 cm) and X-band (4.2 cm) wavelengths in an effort to understand the scattering properties of lunar terrains as a function of bistatic angle. Previous work, at optical wavelengths, has demonstrated that the material properties of lunar regolith can be sensitive to variations in phase (bistatic) angle [1-3]. This sensitivity gives rise to the lunar opposition effect and likely involves contributions from shadow hiding at low phase angles and coherent backscatter near zero phase [1]. Mini-RF bistatic data of lunar materials indicate that such behavior can also be observed for lunar materials at the wavelength scale of an X- and S-band radar these observations are the first time spatially resolved information on this effect have been measured for the Moon at radar wavelengths. The ejecta blankets of ten lunar craters have been observed to date (three of the craters at both X- and S-band), and their Circular Polarization Ratios (CPRs) have been characterized as a function of phase (bistatic) angle. Observing the scattering behavior of continuous ejecta blankets at multiple radar wavelengths can provide information regarding the size/frequency of scatterers emplaced as ejecta, as well as unique insight into the rate of regolith breakdown on the Moon.

Bistatic Operations: Radar observations of planetary surfaces provide important information on the structure (i.e., roughness) and dielectric properties of surface and buried materials [4-7]. These data can be acquired using a monostatic architecture, where a single antenna serves as the signal transmitter and receiver, or they can be acquired using a bistatic architecture, where a signal is transmitted from one location and received at another. The former provides information on the scattering properties of a target surface at zero degree bistatic angle. The latter provides the same information but over a variety of bistatic (phase) angles. NASA's Mini-RF instrument is currently operating in a bistatic architecture with the Arecibo Observatory (AO) in Puerto Rico and the Goldstone DSS-13 antenna in California. The AO serves as the transmitter for S-band operations and DSS-13 serves as the transmitter for X-band operations. Mini-RF serves as the receiver in both cases. This architecture maintains the hybrid dual-polarimetric nature of the Mini-RF instrument [8] and, therefore, allows for the calculation of the Stokes parameters (S_1 , S_2 , S_3 , S_4) that characterize the backscattered signal (and the products derived from those parameters).

Observations: A common product derived from the Stokes parameters is the Circular Polarization Ratio (CPR), or $\mu_c = (S_1 - S_4)/(S_1 + S_4)$. CPR information is commonly used in analyses of planetary radar data [4-7], and is a representation of surface roughness at the wavelength scale of the radar (i.e., surfaces that are smoother at the wavelength scale will have lower CPR values and surfaces that are rougher will have higher CPR values). High CPR values can also serve as an indicator of the presence of water ice [9].

As part of the Mini-RF bistatic observation campaign, CPR information for a variety lunar terrains is being collected over a range of bistatic angles. The first campaign (during LRO extended mission 1) targeted a variety of Copernican-aged impact craters in order to characterize the opposition response of materials known to be rough at radar wavelengths [10]. Patterson *et al.* [10] showed the ejecta properties as a function of bistatic angle for three of these craters: Byrgius A, Kepler, and Bouguer. Both Kepler and Byrgius A exhibited an opposition effect, while Bouguer did not. The opposition responses of Byrgius A and Kepler ejecta lead to increases in CPR of ~40% and 15%, respectively, as bistatic angle approaches 0°. The mean CPR of Byrgius A and Kepler ejecta at bistatic angles, excluding their opposition responses, averages ~20% higher than surrounding materials. The mean CPR of Bouguer ejecta averages ~5% above surrounding materials. Patterson *et al.* [10] suggest that the radar scattering characteristics of the continuous ejecta for these three craters, coupled with age estimates based on crater statistics and geologic mapping, imply a relationship between the opposition response of the ejecta and the age of the crater (i.e., Byrgius A is the youngest of the craters observed and shows the strongest response). Thus, recording the CPR response as a function of bistatic angle may be a way to determine relative age between deposits. Here, we examine the ejecta of 9 Copernican-aged craters that range from 4 to 69 km in diameter (**Table 1**) and document CPR characteristics as a function bistatic angle in order to test that hypothesis. The spatial resolution of the data varied from one observation to another as a function of the viewing geometry, but averaged ~100 m.

Four of the examined craters (Byrgius A, Aristarchus, La Condamine S, and Kepler) exhibit CPR characteristics suggestive of an opposition effect in S-band: higher CPR at lower bistatic (phase) angle (**Figure 1**). X-band observations of Anaxagoras also suggest an opposition surge at low bistatic angle, though relatively constant CPR in S-band at higher bistatic angles. The increase in

CPR occurs near 2–4 degrees bistatic angle. These craters occur in both highlands and mare regions, and are all characterized as young (**Table 1**). Three other examined craters (Bouguer, Harpalus, Anaxagoras) exhibit CPR that remains relatively constant across bistatic angle. This may be for a couple reasons: 1) The craters are older (though most are still Copernican), and so the opposition effect will be less pronounced; or 2) insufficient data have been acquired to characterize the opposition behavior of the crater ejecta. An opposition effect may be present, and not yet observed. Schomberger A, La Condamine S, and Kepler exhibit scattering properties as a function of bistatic angles that differ from the other observed craters, with areas of relatively constant CPR at various CPR values. The oldest crater observed (Hercules, which is classified as Eratosthenian) shows no indication of an opposition response across phase angle

space. Continuing observations are targeting these regions to increase the bistatic angle coverage. Additional study is ongoing to fully characterize the CPR response with viewing geometry for these young craters. All of these targets will also be targeted in X-band.

References: [1] Hapke et al. (1998), *Icarus*, 133, 89-97; [2] Nelson et al. (2000), *Icarus*, 147, 545-558; [3] Piatek et al. (2004), *Icarus*, 171, 531-545. [4] Campbell et al. (2010), *Icarus*, 208, 565-573; [5] Raney et al. (2012), *JGR*, 117, E00H21; [6] Carter et al. (2012), *JGR*, 117, E00H09; [7] Campbell (2012), *JGR*, 117, E06008; [8] Raney, R. K. et al. (2011), *Proc. of the IEEE*, 99, 808-823; [9] Black et al. (2001), *Icarus*, 151, 167-180; [10] Patterson, et al. (2017), *Icarus*, 283, 2-19; [11] Morota et al. (2009) *Met. Planet. Sci.* 44(8), 1115-1120; [12] Koenig et al. (1977) *Proc. LPSC*, 8, p. 555; [13] Baldwin (1985) *Icarus* 61, 63-91; [14] Ulrich (1969) USGS Map I-604(LAC-11).

Table 1. Summary of Mini-RF bistatic observations of young lunar craters examined in this study

Crater	Diameter (km)	Center	Terrain	Age Estimate	Bistatic Angles Observed	Wavelength
Byrgius A	19	24.5°S, 63.7°W	Highlands	48 MY [11]	0.72-13.6	S-band
Kepler	32	8.1°N 38.0°W	Mare	625 MY [12] -1250 MY [13]	1.30-15.2/0.84-4.59	S-band/X-band
Bouguer	22	52.3°N, 35.8°W	Mare	Copernican [14] ~1.2 GY	1.01-5.42	S-band
La Condamine S	4	57.3°N, 25.2°W	Mare	Copernican	0.04-10.3	S-band
Harpalus	39	52.6°N, 43.4°W	Mare	Copernican	5.68-14.9	S-band
Anaxagoras	50	73.4°N, 10.1°W	Highlands	Copernican, 300 My*	4.05-15.9/1.11-6.7	S-band/X-band
Aristarchus	40	23.7°N, 47.4°W	Mare	Copernican	0.02 - 9.28	S-band
Schomberger A	31	78.8°S, 24.4°E	Highlands	Copernican	0.17-17.1	S-band
Hercules	69	46.7°N, 39.1°E	Mare	Eratosthenian	0.004-6.67	S-band

*Age from M. Kirchoff, personal communication

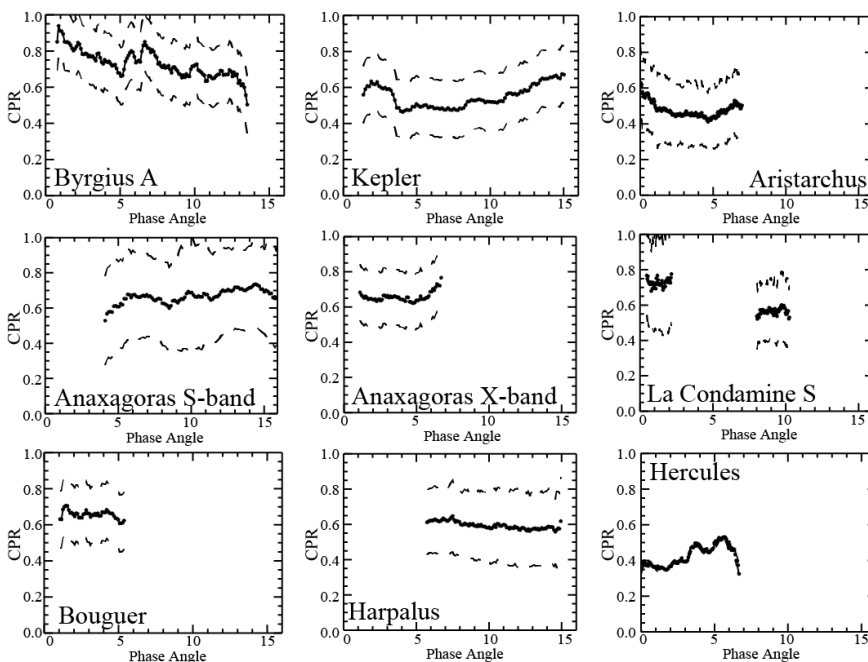


Figure 1. CPR as a function of phase for 8 of the examined craters. Craters here exhibit differences in CPR with bistatic angle; the youngest craters show higher CPR at lower bistatic angles (characteristic of an opposition effect) while (putative) older craters show a flat response. The thick line shows the mean CPR value at each phase angle, while the dashed lines represent one standard deviation from the mean.